Supplemental Information: The mirror-based eyes of scallops demonstrate a light-evoked pupillary response

Hayley V. Miller, Alexandra C. N. Kingston, Yakir L. Gagnon, and Daniel I. Speiser

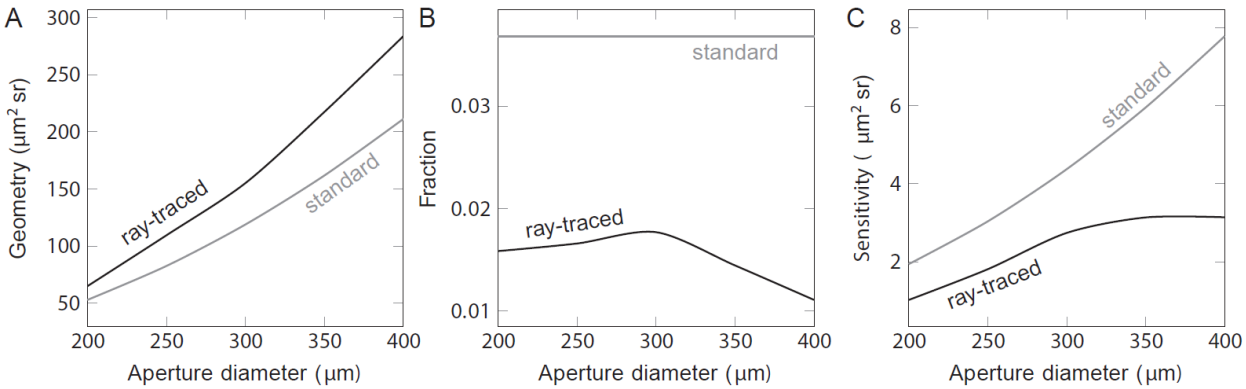

Figure S1. Comparisons between our ray-traced model (in black) and the standard model (in gray) for estimating the sensitivity of the distal retina of the bay scallop *A. irradians* across the range of apertures we observed in our trials.

(A) Geometry, one of the components of sensitivity, describes the amount of available light that terminates on the axial photoreceptor (*i.e.* the receptor centered on the optical axis of the eye). Here, compared to the results of our ray-traced model, we find that the contribution of Geometry to the sensitivity of the distal retina of *A. irradians* is underestimated by the standard model by about 20%. (B), Fraction, the second component of sensitivity, describes the fraction of the available light that is absorbed by the axial photoreceptor. We find that Fraction for the distal retina of *A. irradians* is overestimated by the standard model by a factor of three. Further, we find that the Fraction of light absorbed by the axial photoreceptor decreases with larger apertures because of increased optical aberrations. (C) The Sensitivity of the distal retina of *A.*

irradians is the product of Geometry and Fraction. We find that the predictions from our ray-tracing model are consistently lower than those from the standard model; further, our ray-tracing model indicates that apertures wider than 300 μm do not appear to be associated with increases in sensitivity.

Supplemental Experimental Procedures

Specimen collection and care

For our measurements of light-evoked pupillary responses, we obtained *A. irradians* from Gulf Specimen Marine Lab (Panacea, FL, USA) and *P. magellanicus* from colleagues at the Darling Marine Center (Walpole, ME, USA). For our histological work, we obtained *A. irradians* from Marine Biological Laboratory (Woods Hole, MA, USA). The shell heights of our specimens of *A. irradians* and *P. magellanicus* ranged from 3.90-5.45 and 4.60-4.95 cm, respectively. We kept scallops at the University of South Carolina (Columbia, SC) in a Living Stream System (Frigid Units,Toledo, OH) with recirculating seawater maintained at a temperature of 19.5°C and a salinity of 33 ppt. We conducted experiments on animals within 1-4 weeks of obtaining them.

Documenting light-evoked pupillary responses in scallops

We conducted trials on intact, un-anaesthetized specimens of *A. irradians* and *P. magellanicus* between the hours of 10:00AM and 4:00PM. To restrain scallops while keeping their eyes exposed, we held them in a plastic beaker and fit lengths of plastic tubing between their valves. We positioned the ventral edges of the valves of each scallop at the same height for each trial by adjusting the thickness of a layer of packing

foam at the bottom of the beaker. We filled the beaker with natural seawater to a height of 8 cm (~ 300 mL) so that all animals were covered by the same depth of water in each trial. We performed our experiments at room temperature (~ 20-22°C) and we did not oxygenate animals because the resulting bubbles interfered with our ability to record the pupillary responses of their eyes.

We recorded time-lapse digital images of the pupillary responses of scallops using a Leica S6 D Stereozoom microscope, a Leica DFC3000G microscope camera, and Leica Application Suite V4.4.0. We positioned the microscope and camera on a Nexus Breadboard (Thorlabs, Newton, NJ, USA) set on a ScienceDesk Workstation (Thorlabs). To the breadboard we afixed two light sources, one a 780 nm Infrared (IR) LED Array (Thorlabs) and the other a Cold White LED Array Light Source (Thorlabs). We positioned these light sources symmetrically, 20 cm to either side of the microscope and at an angle of 45° relative to the surface of the breadboard.

To adjust the intensity of the white light source, we used a series of Neutral Density (ND) filters (Thorlabs). As measured from the position of the ventral-most eyes of our test animals, the intensities of white light to which we exposed the eyes of scallops were 1e15 (no filter), 1e14 (ND1), 1e13 (ND2), and 1e12 (ND3) photons/cm^2/sec. To measure absolute irradiance (integrated from 400 to 700 nm), we used a spectrometer system from Ocean Optics (Dunedin, FL, USA) that included a Flame-S-VIS-NIR-ES spectrometer, a QP400-1-UV-VIS optical fiber, and a CC-3 cosine-corrector. We calibrated the absolute spectral response of our system using a HL-3P-CAL calibrated Vis-NIR light source and we operated the spectrometer using Ocean View software.

For each trial, we placed a scallop under the microscope and brought into focus one or several eyes from the ventral region of its mantle. We noted the total magnification at which images were recorded for each trial. We kept the IR LED array turned on for every step of every trial so that we could monitor scallops in the dark with the IR-sensitive microscope camera. For trials involving the constriction of pupils in the light, we dark-adapted animals for at least 45 minutes, and then exposed them to unfiltered light from the white LED array while recording images every five seconds for ten minutes. For trials involving the dilation of pupils in the dark, we dark-adapted animals for at least 45 minutes, exposed them to unfiltered light from the white LED array for ten minutes, and then turned off the white LED array and recorded images every five minutes for 90 minutes in the dark.

For the pupil dilation trials, we recorded responses from 13 eyes from 11 specimens of *A. irradians* and 15 eyes from four specimens of *P. magellanicus*. For the pupil constriction trials with *P. magellanicus*, we recorded responses from 17 eyes from five specimens. We used the same specimens of *P. magellanicus* for both the pupil constriction and pupil dilation trials. For the pupil constriction trials with *A. irradians*, we used separate animals from those that we used for the pupil dilation trials. For the pupil constriction trials involving light intensities of 1e15 (no filter), 1e14 (ND1), 1e13 (ND2), and 1e12 (ND3) photons/cm^2/sec, we recorded the responses of 12 eyes from four individuals, 18 eyes from six individuals, 15 eyes from six individuals, and 16 eyes from six individuals, respectively. For these pupil constriction trials with *A. irradians*, each scallop was tested twice, but no scallop was tested twice on the same day or exposed to the same light treatment more than once.

Using ImageJ [S1], we measured the areas of scallop pupils from our time-lapse images. We converted pixel coordinates to real-world coordinates by calibrating our camera with an ocular micrometer at different magnifications. We prioritized imaging eyes that were aligned so that the plane of their pupil was perpendicular to the camera; however, it is unlikely that any of the eyes were aligned perfectly. We lack data for at least a few time points from most trails because scallops occasionally moved their eyes, covered their eyes with their extensible sensory tentacles, or clapped their valves.

Building a computational model for vision in scallops

To explore the effects of aperture on the sensitivity and resolution of the eyes of scallops, we modified a custom-made ray-tracer described previously [S2, S3]. We implemented our model in Julia, a fast and dynamic programming language for technical computing [S4]. Our new ray-tracing model allows us to estimate sensitivity and resolution while accounting for the absorption coefficients of the distal and proximal photoreceptors and the lengths of their photoreceptive outer segments. These are necessary steps towards calculating sensitivity and resolution for the eyes of scallops because light passes through both retinas twice: the first time as unfocused light and the second time as light focused by the mirror. Our modifications also allowed us to model the eyes of scallops in three dimensions, which was necessary for simulating scenarios involving extended sources and thus required for estimating sensitivity. All the code used in this study is available online (https://github.com/yakir12/Scallops.jl).

We incorporated a factor in our model that accounts for uncertainty about the natural shapes of the eyes of scallop. These small, soft eyes tend to lose their natural

shapes when they are removed from animals and they tend to deform further when they are fixed and/or sectioned. Thus, until we have estimates of morphology from fully-intact eyes still attached to living scallops, we will remain uncertain of the natural dimensions of these visual organs. It is also possible that scallops may be able to voluntarily alter the shapes of their eyes, given that these eyes are found at the tips of short tentacles that contain longitudinal muscle fibers whose contractions allow scallops to bend their eyes away from touch or bright light [S3, S5, S6, S7]. With these considerations in mind, we modeled the eyes of scallops as hydrostats: flexible tubes with constant volumes whose shapes may be controlled by the coordinated contractions of muscle fibers.

For the current paper, we chose to model an eye from *A. irradians* (using the same parameters from [S3]) elongated by 10% along its axial dimension. To preserve the volume of the eye, we shortened it along its transverse dimension by the square root of the inverse of the axial elongation factor (~5%). We chose an elongation factor of 10% because it was associated with a resolution at the distal retina that was consistent with previous estimates of angular resolution in scallops (2°) that were obtained by a variety of approaches, including behavioral trials [S8, S9], electrophysiological experiments [S10], and ray-tracing models [S3, S11, S12]. The effects of aperture on sensitivity and resolution in scallops were similar across a range of elongation factors (7%-15%), demonstrating that the results we report here are robust across a range of morphological possibilities.

Modeling sensitivity and resolution in the scallop eye

Sensitivity is defined as an eye's ability to deliver enough light to its photoreceptors to achieve its finest possible spatial resolution [S13]. The absolute sensitivity of an eye is dictated by the product of two components: 1) the amount of available light that terminates on the photoreceptor centered on the eye's optical axis (hereafter referred to as the "axial photoreceptor") and 2) the Fraction of that light that is absorbed by the axial photoreceptor. These two components may be approximated, respectively, by the Geometry of the eye in question and the absorption coefficient of the axial photoreceptor [S14].

Michael Land elegantly reduced the sensitivity equation by modeling the amount of light available to and absorbed by the axial photoreceptor. Land removed the need to know the distance between an eye and a particular target or that target's area by assuming that all light incident upon the pupil (that originated from a target area subtended by the axial photoreceptor through the eye's nodal point) terminates at the axial photoreceptor (for a helpful description and illustration of these terms see Figure 3 in [S14]). The result of Land's work was the sensitivity equation which was later adapted for white light by Warrant and Nilsson [S15]. Hereafter, we will refer to both Land's and Warrant and Nilsson's versions of the sensitivity equation as the "standard model".

Approximating sensitivity in the manner described above works well for eyes that are accommodated and aberration-free. The eyes of scallops, however, do not lend themselves to this approach, in part because they are defocused. Some of the light incident upon the pupil does not terminate at the axial photoreceptor. In response to this challenge, we developed a new approach for calculating sensitivity using our

computational model for ray-tracing. Because the eyes of scallops are defocused, we started with an unreduced expression of the amount of light incident on their pupils:

$$\frac{L \cdot S_e \cdot S_a}{D^2},$$

where L is the radiance emitted from the Lambertian target, S_e is the target area subtended by the receptor's surface through the system's nodal point, S_a is the area of the aperture, and D is the distance from the pupil to the target. This expression is equivalent to the first component of sensitivity, Geometry.

To calculate S_e we need to calculate the solid angle subtended by the area of the axial photoreceptor at the nodal point of the eye. While the standard model describes that solid angle as the square of the diameter of the receptor divided by the focal length of the eye (*i.e.* the distance between the retina and nodal point), this holds true only for coma-free systems (*i.e.* eyes in which on-axis and off-axis targets are focused identically). Because the eyes of scallops suffer from both LSA (due to the spherical nature of the mirror) and coma (due to the presence of a light-focusing lens and the double passage of the light through the retinas), we calculated this angle directly with our ray-tracer instead. We defined this angle as the FWHM of the angular sensitivity of the axial photoreceptor. By rotating a distant point source around the nodal point and registering the amount of light absorbed at the axial photoreceptor, we described the amount of light absorbed as a function of viewing angle. We used the solid version of the FWHM of that distribution as the angle that subtends the target area, S_e.

In the standard model for estimating the sensitivity of an eye, the second component of sensitivity, the Fraction of light that is absorbed by the axial photoreceptor, is calculated under the assumption that light passes through the center of the outer segment of the receptor along its optical axis. This is an adequate approximation in optical systems with medium to high f-numbers, but the eyes of scallops have remarkably low f-numbers because of their mirror-based optics (as low as 0.54 for the distal retina at the widest aperture we observed). We therefore calculated the Fraction of the light absorbed by the axial photoreceptor by summing all the contributions of rays originating from the extended source and dividing that sum by the number of rays that passed through the pupil.

Assuming an eye is free from aberrations, when in reality it is not, has different implications for the two components of sensitivity, Geometry and Fraction. By assuming an aberration-free system, the standard sensitivity model will tend to underestimate the range of angles from which an axial photoreceptor receives unfocused light. The Geometry component of sensitivity (the first component) is directly affected by the viewing angle of the axial photoreceptor and thus any underestimation of this angle results in an underestimation of the Geometry of the eye. The same assumption has the opposite effect on the Fraction component of sensitivity (the second component): by assuming the system is aberration-free, the standard model of sensitivity will tend to overestimate the Fraction of the available light that has been absorbed by the axial photoreceptor and thus overestimate sensitivity.

To determine whether the underestimation of Geometry or the overestimation of Fraction have the larger net-effect on sensitivity, we compared predictions from our ray-

tracing model to those from the standard model for the Geometry, Fraction, and overall Sensitivity of the distal retina of *A. irradians*. We did not make similar comparisons for the proximal retina because the proximal retina is not positioned in the focal plane of the eye. We found that the contribution of Geometry to the sensitivity of the distal retina is underestimated by the standard model by about 20% (Figure S1A) and that the contribution of Fraction is overestimated by the standard model by a factor of three (Figure S1B). Further, we find that the Fraction of light absorbed by the axial photoreceptor decreases with larger apertures because of increased optical aberrations including LSA. Overall, our ray-tracing model predicts a lower sensitivity for the distal retina than the standard model due to factors including the double passage of light through the retinas, losses of light due to absorption and reflection, coma, LSA, and other aberrations (Figure S1C).

Since the light at the proximal retina was completely unfocused (FWHM of 30-100 degrees), using the standard model for the proximal retina was even more problematic than using it to estimate the sensitivity of the distal retina. We therefore estimated sensitivity for the proximal retina using only our ray-tracing model.

Lastly, we estimated angular resolution at a given retina as the full width at half maximum (FWHM) of the Gaussian distribution of the light intensity across it. While the Point Spread Function (PSF) of the scallop eye is not of a Gaussian nature in either of their retinas, we considered this approximation to be sufficient for the goals of the current study.

Phalloidin-staining of scallop corneas

To identify muscle fibers associated with the dilation and contraction of the pupils of scallops, we used Invitrogen Molecular Probes Rhodamine Phalloidin (ThermoFisher Scientific, Waltham, MA, USA) to stain actin fibers in isolated corneas from *A. irradians*. We fixed eyes from *A. irradians* in 4% formaldehyde in natural seawater for 24 hours at 4°C and then washed them three times in 0.1M phosphate buffered saline (PBS) at room temperature. Next, to view the interior surfaces of corneas and their surrounding tissues, we cut off the distal hemispheres of fixed eyes and removed the lenses contained within them. We counterstained these isolated corneas by blocking them in solutions of PBS + 0.3% Triton-100 + 10% normal goat serum for 1 hour at room temperature, incubating them in phalloidin (diluted 1:1000 in blocking solution) overnight at 4°C, and washing them three times for 20 minutes in PBS. We mounted stained corneas on slides with DAPI Fluoromount (Southern Biotech, Birmingham, AL, USA), imaged counterstained corneas with a confocal microscope (Leica, SP8), and analyzed the resulting images using Fiji [S1].

Acknowledgements

For their help with this project, the authors thank Skylar Young Bayer, Jeff Twiss, Dan-E. Nilsson, Eric Warrant, Sönke Johnsen, and Michael Land. Support for the authors was provided by IOS Award no. 1457148 from the National Science Foundation (to D.I.S), a Magellan Scholar Award from the University of South Carolina and a Science Undergraduate Research Fellowship from the South Carolina Honors College (to

H.V.M.), and an Individual Fellowships MSCA-VINNOVA no. 2017-03023 from the European Commission (to Y.L.G.).

Author contributions

H.V.M. documented pupillary responses, H.V.M. and A.C.N.K. visualized actin fibers, Y.L.G. developed and implemented the ray-tracing model, D.I.S. designed the project and oversaw it, and all contributed to analyzing data and writing the manuscript.

Supplemental References

S1. Schindelin, J., Arganda-Carreras, I., Frise, E., Kaynig, V., Longair, M., Pietzsche, T., Preibisch, S., Rueden, C., Saalfeld, S., Schmid, B., *et al*. (2012) Fiji: an open-source platform for biological-image analysis. Nature Methods 9, 676-682.

S2. Gagnon, Y. L., Speiser, D. I., and Johnsen, S. (2014) Simplifying numerical ray tracing for characterization of optical systems. Applied Optics 53, 4784-4790.

S3. Speiser, D. I., Gagnon, Y. L., Chhetri, R. K., Oldenburg, A. L., and Johnsen, S. (2016) Examining the effects of chromatic aberration, object distance, and eye shape on image-formation in the mirror-based eyes of the bay scallop *Argopecten irradians*. Integrative and Comparative Biology 56, 796-808.

S4. Bezanson, J., Edelman, A., Karpinski, S., and Shah, V. B. (2017) Julia: A fresh approach to numerical computing. SIAM Review 59, 65-98.

S5. Patten, W. (1886) Eyes of molluscs and arthropods. Mittheilungen aus der Zoologischen Station zu Neapel 6, 542-756.

S6. Dakin, W. J. (1910) The eye of *Pecten*. Quarterly Journal of Microscopical Science 55, 49-112.

S7. Barber, V. C., Evans, E. M., Land, M. F. (1967) The fine structure of the eye of the mollusc *Pecten maximus*. Zeitschrift für Zellforschung und Mikroskopische Anatomie 76, 295-312.

S8. Buddenbrock, W. von and Moller-Racke, I. (1953) Uber den lichtsinn von *Pecten*. Pubblicazioni della Stazione Zoologica die Napoli 24, 217-245.

S9. Speiser, D. I., and Johnsen, S. (2008) Comparative morphology of the concave mirror eyes of scallops (Pectinoidea). American Malacological Bulletin 26, 27-33.

S10. Land, M. F. (1966) Activity in the optic nerve of *Pecten maximus* in response to changes in light intensity and to pattern and movement in the optical environment. The Journal of Experimental Biology 45, 83-99.

S11. Land, M. F. (1965) Image formation by a concave reflector in the eye of the scallop, *Pecten maximus*. The Journal of Physiology 179, 138-153.

S12. Palmer, B. A., Taylor, G. J., Brumfeld, V., Gur, D., Shemesh, M., Elad, N., Osherov, A., Oron, D., Weiner, S., and Addadi, L. (2017) The image forming mirror in the eye of the scallop. Science 358, 1172-1175.

S13. Land, M. F. and Nilsson, D.-E. (2012) Animal Eyes (New York, Oxford University Press).

S14. Land, M. F. (1981) Optics and vision in invertebrates. In Handbook of Sensory Physiology 6B: Vision in Invertebrates, H. Autrum, ed. (Berlin, Springer Verlag), pp. 471-594.

S15. Warrant, E. J. and Nilsson, D.-E. (1998) Absorption of white light in photoreceptors. Vision Research 38, 195-207.